THE JOURNAL OF BIOLOGICAL CHEMISTRY
Vol. 265, No. 15, Issue of May 25, pp. 8533-8541, 1990
Printed in U.S.A.

Spectroscopic Characterization of the Novel Iron-Sulfur Cluster in *Pyrococcus furiosus* Ferredoxin*

(Received for publication, December 27, 1989)

Richard C. Conover, Andrzej T. Kowal‡, Weiguang Fu, Jae-Bum Park, Shigetoshi Aono, Michael W. W. Adams, and Michael K. Johnson§

From the School of Chemical Sciences and Center for Metalloenzyme Studies, University of Georgia, Athens, Georgia 30602

Pyrococcus furiosus **ferredoxin is the only known example of a ferredoxin containing a single [4Fe-4S] cluster that has non-cysteinyl ligation of one iron atom, as evidenced by the replacement of a ligating cysteine residue by an aspartic acid residue in the amino acid sequence. The properties of the iron-sulfur cluster in both the aerobically and anaerobically isolated ferredoxin have been characterized by EPR, magnetic circular dichroism, and resonance Raman spectroscopies. The anaerobically isolated ferredoxin contains a [4Fe-4S]$^{+,2+}$ cluster with anomalous properties in both the oxidized and reduced states which are attributed to aspartate and/or hydroxide coordination of a specific iron atom. In the reduced form, the cluster exists with a spin mixture of $S = 1/2$ (20%) and $S = 3/2$ (80%) ground states. The dominant $S = 3/2$ form has a unique EPR spectrum that can be rationalized by an $S = 3/2$ spin Hamiltonian with $E/D = 0.22$ and $D = +3.3 \pm 0.2$ cm^{-1}. The oxidized cluster has an $S = 0$ ground state, and the resonance Raman spectrum is characteristic of a [4Fe-4S]$^{2+}$ cluster except for the unusually high frequency for the totally symmetric breathing mode of the [4Fe-4S] core, 342 cm^{-1}. Comparison with Raman spectra of other [4Fe-4S]$^{2+}$ centers suggests that this behavior is diagnostic of anomalous coordination of a specific iron atom. The iron-sulfur cluster is shown to undergo facile and quantitative [4Fe-4S] ↔ [3Fe-4S] interconversion, and the oxidized and reduced forms of the [3Fe-4S] cluster have $S = 1/2$ and $S = 2$ ground states, respectively. In both redox states the [3Fe-4S]$^{0,+}$ cluster exhibits spectroscopic properties analogous to those of similar clusters in other bacterial ferredoxins, suggesting non-cysteinyl coordination for the iron atom that is removed by ferricyanide oxidation. Aerobic isolation induces partial degradation of the [4Fe-4S] cluster to yield [3Fe-4S] and possibly [2Fe-2S] centers. Evidence is presented to show that only the [4Fe-4S] form of this ferredoxin exists *in vivo*.**

A novel ferredoxin (Fd)[1] that functions as the electron donor to hydrogenase has been isolated from the hyperthermophilic archaebacterium *Pyrococcus furiosus* (1). It is a monomeric protein of molecular weight 7500, containing four non-heme iron atoms and five cysteinyl residues[2] which exhibits some remarkable and unusual properties in comparison with other bacterial [4Fe-4S] ferredoxins. For example, it is stable at 95 °C for at least 12 h in contrast to other "thermostable" ferredoxins that are rapidly denatured at 85 °C (1), and it has an atypical arrangement of cysteinyl residues: X_{10}-Cys-X_2-Asp-X_2-Cys-X_3-Cys-Pro-X_{25}-Cys-X_7-Cys-Pro-X_9.[2] The arrangement of cysteine 11, 17, and 56 is analogous to that of other [4Fe-4S] ferredoxins, but an aspartate (Asp^{14}) replaces the cysteinyl residue that would customarily complete the cluster ligation. Consequently it is probable that one iron atom in the [4Fe-4S] cluster is coordinated by aspartate and/or H_2O or OH^-. Of the more than 30 4Fe and 8Fe ferredoxin sequences known (2), the replacement of 1 coordinating cysteine by an aspartate is only evident in ferredoxins from *Desulfovibrio vulgaris* (3), *Desulfovibrio africanus* (4), *Thermoplasma acidophilum* (5), and *Sulfolobus acidocaldarius* (6). However, all of these are 8Fe ferredoxins, leaving the *P. furiosus* protein as the only 4Fe ferredoxin with incomplete cysteinyl coordination to its single [4Fe-4S] cluster. Site-differentiated [4Fe-4S] clusters with non-cysteinyl coordination of one iron atom are of considerable current interest in Fe-S cluster chemistry and biochemistry (7, 8). For example one iron in the [4Fe-4S] cluster of aconitase is coordinated by oxygen derived from solvent H_2O or OH^- (9) and is the site of substrate binding and isomerization (10). Furthermore, the unusual properties of nitrogenase P-clusters (11) and Fe-hydrogenase H-clusters (12) are also likely to be a consequence of non-cysteinyl coordination of one or more iron atoms.

In this study we report on the characterization of the [4Fe-4S] cluster in *P. furiosus* Fd using the combination of low temperature EPR, magnetic circular dichroism (MCD), and resonance Raman spectroscopies. The results reveal anomalous spectroscopic and magnetic properties for the [4Fe-4S]$^{1+,2+}$ cluster in both the oxidized and reduced states compared with similar centers in other bacterial ferredoxins and facile cluster interconversion between [4Fe-4S] and [3Fe-4S] forms. Taken together these results provide convincing evi-

* This work was supported by National Science Foundation Grants DMB8796212 (to M. K. J.) and DMB8805255 (to M. W. W. A.), National Institutes of Health Grant GM33806 (to M. K. J.), United States Department of Energy Grant FG09-88ER13901 (to M. W. W. A.), and Petroleum Research Fund Grant ACS-PRF 21925-AC4,3 (to M. W. W. A.). The costs of publication of this article were defrayed in part by the payment of page charges. This article must therefore be hereby marked "*advertisement*" in accordance with 18 U.S.C. Section 1734 solely to indicate this fact.

‡ Present address: Institute of Inorganic Chemistry, Technical University of Wroclaw, Wroclaw 50-370, Poland.

§ To whom correspondence should be sent: Dept. of Chemistry, University of Georgia, Athens, GA 30602.

[1] The abbreviations used are: Fd, ferredoxin; MCD, magnetic circular dichroism; W, watt(s), Hepes, 4-(2-hydroxyethyl)-1-piperazineethanesulfonic acid; Hepps, 4-(2-hydroxyethyl)-1-piperazinepropanesulfonic acid; Mops, 4-morpholinepropanesulfonic acid; Mes, 4-morpholinethanesulfonic acid; Ches, 2-(*N*-cyclohexylamino)ethanesulfonic acid; Caps, 3-(cyclohexylamino)-1-propanesulfonic acid; T, tesla.

[2] E. Eccleston, J.-B. Park, M. W. W. Adams, and J. B. Howard, manuscript in preparation.

dence for non-cysteinyl coordination of the iron atom that is removed on formation of the [3Fe-4S] cluster. Moreover, since *P. furiosus* Fd contains only a single cluster, this protein will be very useful in investigating the properties of both site-differentiated [4Fe-4S] clusters and mixed metal [M3Fe-4S] clusters (where M = nickel,[3] molybdenum, tungsten, and vanadium) in a biological environment.

MATERIALS AND METHODS

P. furiosus Fd was isolated under both anaerobic and aerobic conditions as described previously (1). The protein concentrations used in quantifying the MCD and EPR spectra are based on a revised molecular weight of 7,500 (from amino acid sequence analysis)[2] and were determined by the method of Lowry *et al.* (13) using the apoprotein prepared by precipitation with trichloroacetic acid (1). This molecular weight leads to a molar absorption coefficient at 390 nm, ϵ_{390} = 17,000 M^{-1} cm^{-1} for air-oxidized samples of anaerobic preparations. Anaerobic samples were isolated in the presence of 2 mM sodium dithionite, and anaerobic sample handling was carried out in a Vacuum Atmospheres glove box (<1 ppm O_2) under argon.

MCD spectra were recorded using Jasco J-500C spectropolarimeter mated to an Oxford Instruments SM-3 super-coil superconducting magnet. The experimental protocols for measuring MCD spectra and magnetization curves over the temperature range 1.5–300 K with magnetic fields up to 5 tesla have been described elsewhere (14). Samples for variable temperature MCD studies contained 50% (v/v) glycerol to facilitate formation of a glass on freezing. EPR spectra were recorded using an IBM ER-200D spectrometer interfaced to a Bruker 1600 computer and fitted with an Oxford Instruments ESR-9 flow cryostat (4.2– to 300 K). Absolute sample temperatures were assessed by replacing the sample with an EPR tube containing a calibrated silicon diode resistance thermometer (Lake Shore Cryogenics) immersed in frozen buffer solution, without adjusting the helium flow. Spin quantitations were performed under nonsaturating conditions using 1 mM Cu(EDTA) as the standard and the procedures developed by Aasa and Vänngård (15). Raman spectra were recorded with an Instruments SA U1000 spectrometer fitted with a cooled RCA 31034 photomultiplier tube using lines from a Coherent Innova 100 10-watt argon ion laser. Scattering was collected at 90° from the surface of a frozen droplet of protein on the cold finger of an Air Products Displex model CSA-202E closed cycle refrigerator. Band positions were calibrated using the excitation frequency and the principal bands of CCl_4 and Na_2SO_4 and are accurate to ±1 cm^{-1}. Further details of the Raman spectrometer and the procedures for obtaining low temperature spectra of frozen anaerobic protein solutions are given in Ref. 16. Room temperature UV-visible absorption spectra were recorded using a Hewlett-Packard 8452 spectrophotometer.

RESULTS

Spectroscopic studies were carried out on samples isolated anaerobically in the presence of 2 mM sodium dithionite and aerobically using the same purification procedures. Since aerobic purification was found to induce partial Fe-S cluster degradation (see below), the results for these two types of preparation are presented separately.

Anaerobically Purified Ferredoxin

Dithionite-reduced—EPR spectra of the anaerobically prepared ferredoxin in the presence and absence of 50% (v/v) glycerol are shown in Fig. 1. The spectra are composed of low field resonances around g = 5 which are indicative of an S = 3/2 spin system and a rhombic S = 1/2 resonance, g = 2.10, 1.87, 1.80. As noted previously (1), the S = 1/2 resonance is broader and undergoes more rapid relaxation than EPR signals from S = 1/2 $[4Fe\text{-}4S]^+$ clusters in other bacterial ferredoxins, such that it is not observable at temperatures above 15 K. The temperature dependence of the low field S = 3/2 resonances is shown in Fig. 2 for the sample in the absence

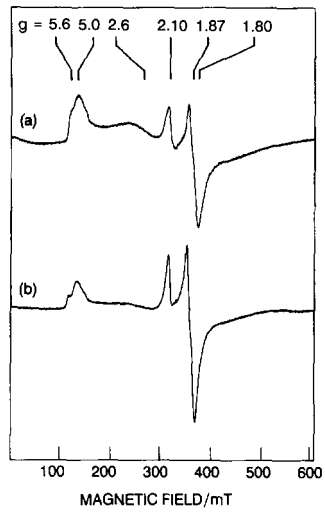

FIG. 1. **EPR spectra of dithionite-reduced anaerobically purified *P. furiosus* ferredoxin.** *a*, anaerobically purified ferredoxin (0.75 mM) in 50 mM Tris/HCl buffer (pH 7.8), 2 mM sodium dithionite, with 50% (v/v) glycerol. *b*, anaerobically purified ferredoxin (0.50 mM) in 50 mM Tris/HCl buffer (pH 7.8), 2 mM sodium dithionite. Conditions of measurement are the same for both samples: microwave power, 10 mW; temperature, 8 K; modulation amplitude, 0.5 mT; microwave frequency, 9.41 GHz.

of glycerol. The relative intensities of the absorption-shaped features centered at g = 5.6 and 5.0 are strongly temperature dependent, with the former becoming more pronounced at higher temperatures. These resonances are, therefore, attributed to two different Kramers doublets that are split by a finite energy at zero field. The energy separation, Δ, between these doublets was assessed by assuming a Boltzmann population distribution and plotting the natural logarithm of the ratio of the intensities of the g = 5.6 and 5.0 features against the reciprocal of the absolute temperature (see *inset* in Fig. 2). This plot is linear within experimental error, and the slope (=Δ/k, where k is the Boltzmann constant) affords an estimate of Δ = 7.0 ± 0.4 cm^{-1}. Since the zero-field splitting is much greater than the Zeeman interaction, it is appropriate to analyze the spectrum in terms of effective g-values for each doublet of an S = 3/2 ground state, using a spin Hamiltonian, H_e, with D and E as the axial and rhombic splitting parameters and an isotropic g-tensor, g_0 (17).

$$H_e = D[S_z^2 - S(S + 1)/3] + E(S_x^2 - S_y^2) + g_0\beta\mathbf{H}\cdot S$$

The observed g-values are consistent with this type of analysis. For example, E/D = 0.22 and g_0 = 1.98 affords doublets with effective g-values of g_x = 2.61, g_y = 5.05, g_z = 1.72 and g_x = 1.35, g_y = 1.09, g_z = 5.68. A broad derivative-shaped resonance centered at g = 2.6 appears concomitant with the g = 5.0 feature as the temperature is lowered. Broad high field resonances with g < 2 are observable but too diffuse to allow accurate assessment of the effective g-values. The temperature dependence of the EPR dictates that the doublet with the low field feature at g = 5.0 lies lowest in energy which corresponds to D > 0. Using the relationship $\Delta = 2D(1 + 3(E/D)^2)^{1/2}$ (17), we estimate that D = +3.3 + 0.2 cm^{-1}.

Quantitation of the S = 1/2 resonance in isolation *versus* a Cu(EDTA) standard under nonsaturating conditions gave values ranging from 0.20 and 0.24 spins/molecule (four different preparations). The S = 3/2 resonance was quantified against the indigenous S = 1/2 resonance using the method developed by Aasa and Vänngård (15) for assessing the spin quantitation based on the integrated area of a well separated, absorption-shaped component of a rhombic signal. The low

[3] R. C. Conover, J.-B. Park, M. W. W. Adams, and M. K. Johnson, manuscript submitted to *J. Am. Chem. Soc.*

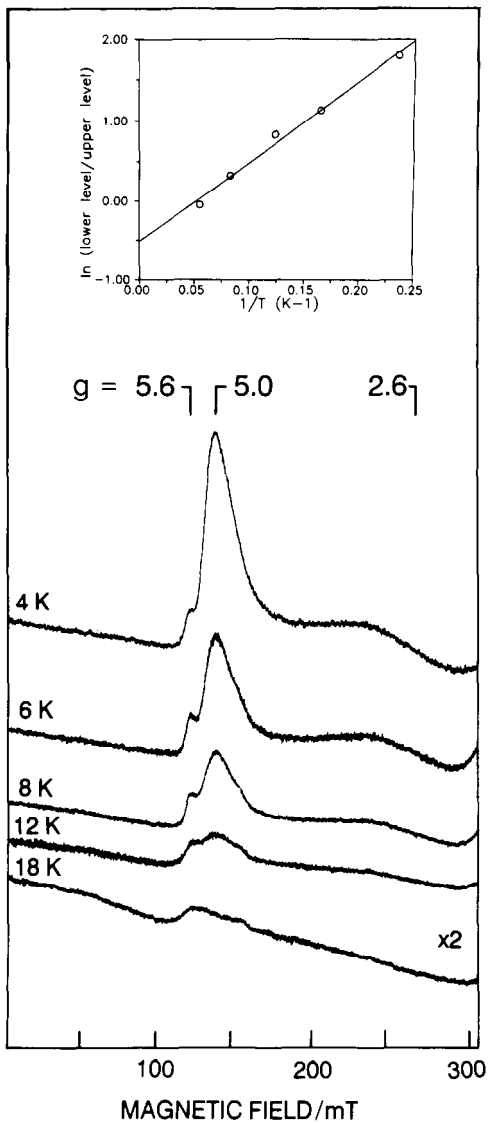

FIG. 2. **Effect of temperature on the $S = 3/2$ resonances of dithionite-reduced anaerobically purified *P. furiosus* ferredoxin.** Sample conditions are as described in Fib. 1*b*. Conditions of measurement: microwave power, 50 mW, modulation amplitude, 0.5 mT; microwave frequency, 9.41 GHz; temperatures as indicated. *Inset*, plot of the natural logarithm of the ratio of the amplitudes at $g = 4.96$ and $g = 5.55$ *versus* the reciprocal of the absolute temperature.

field features at $g = 5.6$ and 5.0 were simulated as overlapping Gaussian-shaped bands and integrated separately under non-saturating conditions (8 K and 10 mW). After correction for the population of the two doublets, the agreement between the values obtained for each of the two bands was remarkably good considering the approximations involved, 0.90 ± 0.10 spins/molecule and 0.74 ± 0.10 spins/molecule for the $g = 5.6$ and 5.0 features, respectively. Average values for the spin quantitations, 0.22 spins/mol and 0.82 spins/mol for the $S = 1/2$ and $S = 3/2$ resonances, respectively, are given in Table I. Within experimental error, these values add up to 1 spin/molecule suggesting that the $[4Fe\text{-}4S]^+$ cluster exists as a mixture of species with $S = 1/2$ and $S = 3/2$ ground states. The form of the spectrum and the relative intensity of the $S = 1/2$ and $S = 3/2$ features were unaffected by pH in the range 6.0–10.5, the nature of the buffering medium (Hepes, Tris, Hepps, Mops, Ches, and Caps, all 100 mM), or the addition of 0.4 M urea. The addition of 50% (v/v) glycerol results in slight broadening of the $S = 3/2$ resonance and shift of the spin mixture in favor of the $S = 3/2$ species (see

TABLE I

EPR spin quantitations for P. furiosus ferredoxin

The values quoted are the average of least three independent determinations. The estimated errors are ±10% for $S = 1/2$ signals and ±20% for $S = 3/2$ signals.

	$[3Fe\text{-}4S]^+$ $S = 1/2$[b]	$[4Fe\text{-}4S]^+$ $S = 1/2$[c]	$[4Fe\text{-}4S]^+$ $S = 3/2$[d]
Anaerobically prepared			
Dithionite-reduced		0.22	0.82
Dithionite-reduced + glycerol		0.08	1.00
Thionine-oxidized	<0.03		
Air-oxidized	<0.05		
Ferricyanide-oxidized	1.00		
Aerobically prepared			
As prepared	0.25		
Dithionite-reduced + glycerol		0.15	0.70

[b] $g_\parallel = 2.02$ and $g_\perp = 1.95$. Quantitations carried out at 8 K and 10-μW microwave power.

[c] $g = 2.10, 1.87, 1.80$. Quantitations carried out at 8 K and 1-mW microwave power.

[d] Quantitations are the average of values obtained for the low field, absorption-shaped features at $g = 5.6$ and 5.0. See "Results" for details.

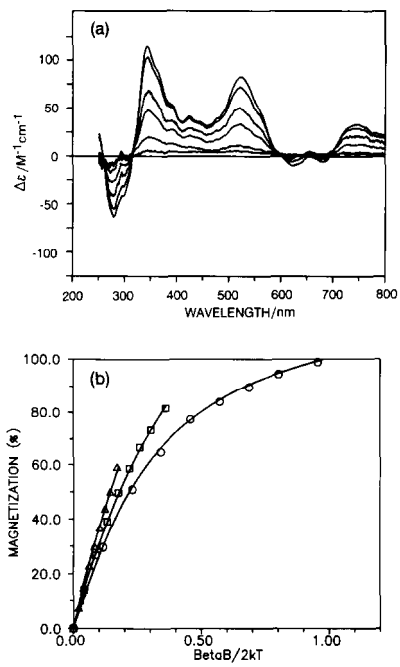

FIG. 3. **Variable temperature MCD spectra and magnetization plot of dithionite-reduced anaerobically purified *P. furiosus* ferredoxin.** Anaerobically purified ferredoxin (0.35 mM) in 50 mM Tris/HCl buffer (pH 7.8), 2 mM sodium dithionite, with 50% (v/v) glycerol. *a*, MCD spectra at 4.5 T and 1.60 K, 4.22 K, 9.1 K, 14.8 K, 50 K, and 76 K (MCD intensity at all wavelengths increases with decreasing temperature). *b*, MCD magnetization data at 522 nm. Magnetic fields are between 0 and 4.5 T; temperatures, ○, 1.63 K; □, 4.22 K; △, 8.9 K.

Fig. 1). By using the same quantitation procedure, the $S = 1/2$ and $S = 3/2$ resonances for samples containing glycerol accounted for 0.08 spins/molecule and 1.00 spins/molecule, respectively (see Table I). Therefore, samples for MCD spectroscopy were at least 90% in the $S = 3/2$ form.

MCD spectra recorded at 4.5 T for temperatures in the range 1.60–76 K are shown in Fig. 3*a*. Identical spectra were obtained for samples in 100 mM Mes buffer (pH 5.9), 100 mM Hepps buffer (pH 7.8), and 100 mM glycine/NaOH (pH 10.5). Biological $[4Fe\text{-}4S]^+$ clusters with $S = 1/2$ ground states give rise to characteristic low temperature MCD spectra consisting of broad positive bands centered between 700 and 760 nm and

520 and 560 nm, multiple positive bands in the region between 350 and 550 nm, and pronounced negative features between 580 and 700 nm and 300 and 330 nm (12). Recent studies in this laboratory involving nitrogenase Fe-protein and a range of synthetic clusters each having $[4Fe\text{-}4S]^+$ centers with predominantly $S = 3/2$ or $S = 1/2$ ground states (18)[4] show that the most pronounced change in the MCD spectrum accompanying an $S = 1/2$ to $S = 3/2$ spin state change is the loss of the pronounced negative band between 580 and 780 nm. Based on these studies, we conclude that the form and intensity of the MCD spectra shown in Fig. 3*a* are indicative of approximately one $[4Fe\text{-}4S]^+$ with an $S = 3/2$ ground state. An $S = 3/2$ ground state for the $[4Fe\text{-}4S]^+$ cluster is also manifest in MCD magnetization data collected at 522 nm (Fig. 3*b*). The nested set of plots (*i.e.* data obtained by varying the magnetic field at different fixed temperatures lie on separate curves) is a consequence of the Boltzmann population and/or field-induced mixing of zero-field components of an $S > 1/2$ ground state (14).

Thionine- or Air-oxidized—After removal of excess sodium dithionite by gel filtration, samples were oxidized by a small excess of thionine under anaerobic conditions or by exposure to air and investigated by EPR, MCD, and resonance Raman spectroscopies. The EPR spectra consisted of a weak $S = 1/2$ resonance, $g_\parallel = 2.02$ and $g_\perp = 1.95$, which accounted for <0.03 spins/molecule and <0.05 spins/molecule for the thionine-oxidized and air-oxidized samples, respectively. The intensity of the EPR signal was not significantly increased by incubating the protein at 23 °C for 7 days under aerobic conditions. Both the dye- and air-oxidized samples exhibited very weak temperature-dependent MCD features arising from the EPR-detectable $S = 1/2$ species, and the form of the spectra enabled assignment to a trace component of $[3Fe\text{-}4S]^+$ clusters. (The MCD characteristics of $[3Fe\text{-}4S]^+$ clusters in the ferricyanide-treated ferredoxin are discussed below.) The MCD and EPR studies combined suggest that almost all of the iron in the thionine-oxidized ferredoxin is in the form of diamagnetic ($S = 0$) $[4Fe\text{-}4S]^{2+}$ clusters. This conclusion was confirmed by resonance Raman studies.

The resonance Raman spectrum of the thionine-oxidized ferredoxin obtained with 457.9 nm excitation is shown in Fig. 4*a*. Identical spectra were observed for air-oxidized samples. The frequences[5] and relative intensities of the observed bands are very similar to those of $[4Fe\text{-}4S]^{2+}$ clusters in oxidized *Clostridium pasteurianum* Fd and reduced *Chromatium vinosum* high potential iron-sulfur protein (19, 20). Table II compares the frequencies of the Fe-S stretching modes of oxidized *C. pasteurianum* Fd with oxidized *P. furiosus* Fd. The former have been rigorously assigned under effective D_{2d} symmetry by extensive studies of synthetic analog complexes, ^{34}S and ^{54}Fe isotope shifts, and normal mode calculations (20). To a first level of approximation, the vibrational modes can be classified as primarily involving terminal (iron-cysteinyl) or bridging Fe-S stretching, and the observed bands in *P. furiosus* Fd are assigned on this basis by analogy with *C. pasteurianum* Fd. For the terminal modes, only one band at 363 cm^{-1} was observed for *P. furiosus* Fd compared with a pair of bands at 363 and 351 cm^{-1} for *C. pasteurianum* Fd. However, precedent for this type of behavior is found in *C. vinosum* high potential iron-sulfur protein (20), where it is

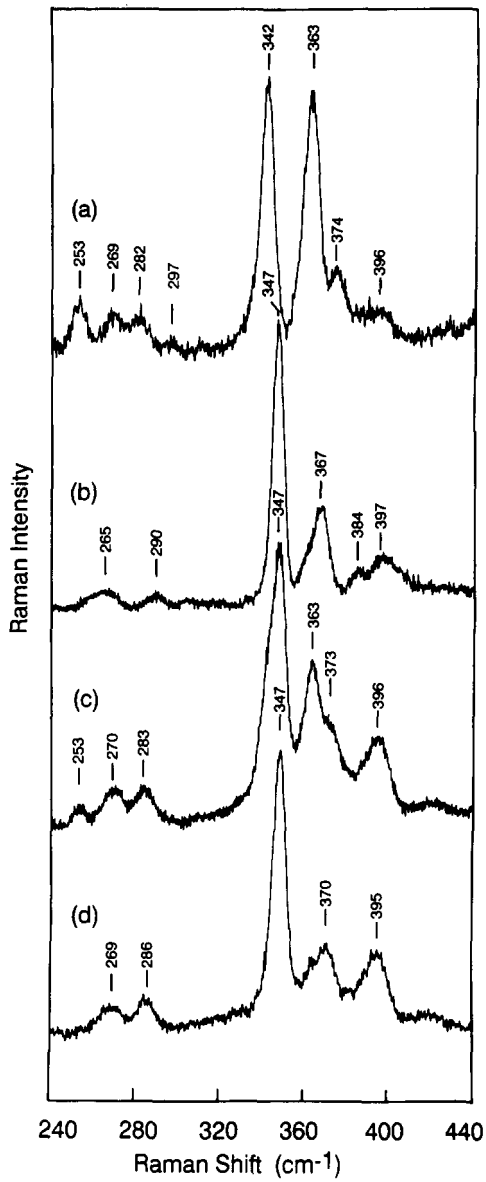

FIG. 4. **Resonance Raman spectra of *P. furiosus* ferredoxin.** *a*, thionine-oxidized anaerobically purified ferredoxin. *b*, ferricyanide-oxidized anaerobically purified ferredoxin. *c*, aerobically purified ferredoxin. *d*, difference spectrum: *c* minus *a*. Samples were all ~4 mM and were in 100 mM Tris/HCl buffer (pH 7.8). Anaerobically purified samples were oxidized by incubation with a 5-fold excess of the oxidizing agent for 15 min at room temperature. Excess oxidant was removed using a Sephadex G-25 column prior to sample concentration. Conditions of measurement: excitation wavelength, 457.9 nm; laser power at sample, 30 mW; sample temperature, 16 K; spectral band width, 6 cm^{-1}; photon counting for 1 s every 0.2 cm^{-1} for each scan; spectra are the sum of eight scans.

interpreted in terms of a more symmetric cluster approaching idealized T_d geometry. The most significant difference in the Raman spectrum of oxidized *P. furiosus* Fd lies in the frequency of the totally symmetric bridging vibration (342 cm^{-1}) which is shifted to higher energy by 4–5 cm^{-1} compared with $[4Fe\text{-}4S]^{2+}$ clusters in bacterial ferredoxins and high potential iron-sulfur proteins. As discussed below, abnormally high frequencies for the totally symmetric bridging vibration appear to be a characteristic of $[4Fe\text{-}4S]^{2+}$ clusters that are site differentiated via different terminal ligation of a specific iron atom.

Ferricyanide-oxidized—Oxidation of the anaerobically prepared ferredoxin with a 5-fold stoichiometric excess of ferricyanide produced results very different from thionine or air

[4] M. K. Johnson, Y. A. Onate, M. G. Finnegan, and B. J. Hales, manuscript in preparation.

[5] The Fe-S vibrational frequencies given in this work are for frozen protein solutions at 17 or 77 K. Although the spectral features remain unchanged, the observed frequencies are generally shifted to higher energy by 1–2 cm^{-1} in frozen solutions compared with room temperature spectra.

TABLE II

Comparison of the Fe-S stretching frequencies (cm^{-1}) of [4Fe-4S]$^{2+}$ and [3Fe-4S]$^{+}$ clusters in C. pasteurianum and P. furiosus ferredoxins

[4Fe-4S]$^{2+}$		[3Fe-4S]$^{+}$	
C. pasteurianum Fd[a]	*P. furiosus* Fd[b]	*C. pasteurianum* Fd[c]	*P. furiosus* Fd[d]
Mainly terminal ν(Fe-S)			
395 (3.9)[e]	396	392 (0)	397
363 (2.0)	363	385 (0)	384
351 (0.7)		368 (0)	367
Mainly bridging ν(Fe-S)			
380 (5.6)	374	347 (7)	347
338 (7.0)	342	285 (4)	290
298 (4.9)	295	267 (6)	265
276 (4.5)	282		
266 (4.0)	269		
251 (6.2)	253		

[a] Oxidized *C. pasteurianum* Fd in frozen solution at 77 K. Taken from Ref. 20.

[b] Thionine-oxidized *P. furiosus* Fd in frozen solution at 17 K.

[c] Ferricyanide-oxidized *C. pasteurianum* Fd in frozen solution at 77 K. Taken from Ref. 21.

[d] Ferricyanide-oxidized *P. furiosus* Fd in frozen solution at 17 K.

[e] Numbers in parentheses are downshifts upon ^{34}S substitution of bridging sulfur atoms. Taken from Refs. 20 and 21.

oxidation. As evidenced by EPR, variable temperature MCD, and resonance Raman studies (see Figs. 4*b* and 5), ferricyanide oxidation results in quantitative oxidative degradation of $S = 0$ [4Fe-4S]$^{2+}$ centers to yield $S = 1/2$ [3Fe-4S]$^{+}$ clusters. The EPR spectrum (see Fig. 5*c*) comprises a fast relaxing, axial resonance, $g_{\parallel} = 2.02$ and $g_{\perp} = 1.95$, that is only observable at temperatures below 30 K and quantifies to 1.0 spin/molecule (see Table I). Similar EPR signals, although varying in the extent of g-value anisotropy and relaxation properties, have been observed for all known [3Fe-4S]$^{+}$ clusters (23, 24). The low temperature MCD spectrum also provides a method of determining cluster type. Between 550 and 300 nm all known [3Fe-4S]$^{+}$ clusters exhibit a similar pattern of temperature-dependent MCD bands which is quite distinct from the spectra exhibited by any other type of paramagnetic Fe-S cluster (23–27). Based on this criterion, the paramagnetic cluster in the ferricyanide-oxidized Fd is clearly of the [3Fe-4S]$^{+}$ type, and the intensity of MCD spectrum in this region is consistent with complete and quantitative [4Fe-4S] to [3Fe-4S] cluster conversion. MCD magnetization data (see Fig. 5*b*) confirm that the MCD transitions originate from the same $S = 1/2$ ground state that is responsible for the EPR signal.

The resonance Raman spectrum of ferricyanide-oxidized *P. furiousus* Fd (see Fig. 4*b*) confirms that the [3Fe-4S]$^{+}$ cluster is structurally analogous to similar clusters in other bacterial ferredoxins. Raman investigations of [3Fe-4S]$^{+}$ clusters in ferredoxins from *C. pasteurianum, Desulfovibrio gigas, Azotobacter vinelandii,* and *Thermus thermophilus* established the existence of a common [3Fe-4S] core structure (21). The [3Fe-4S]$^{+}$ clusters in these ferredoxins exhibit three bands associated primarily with Fe-S bridging modes at 262–267 cm^{-1}, 285–290 cm^{-1}, and 347–348 cm^{-1}, and two or three Fe-S-terminal modes between 360 and 400 cm^{-1}. Both the frequencies and relative intensities of the Raman bands of ferricyanide-oxidized *P. furiosus* Fd conform to the general picture established for [3Fe-4S]$^{+}$ clusters in these bacterial ferredoxins. The closest correspondence is with the [3Fe-4S]$^{+}$ cluster in ferricyanide-treated *C. pasteurianum* Fd, in which there is a direct one-to-one correspondence of spectral features with only minor frequency differences (see Table II).

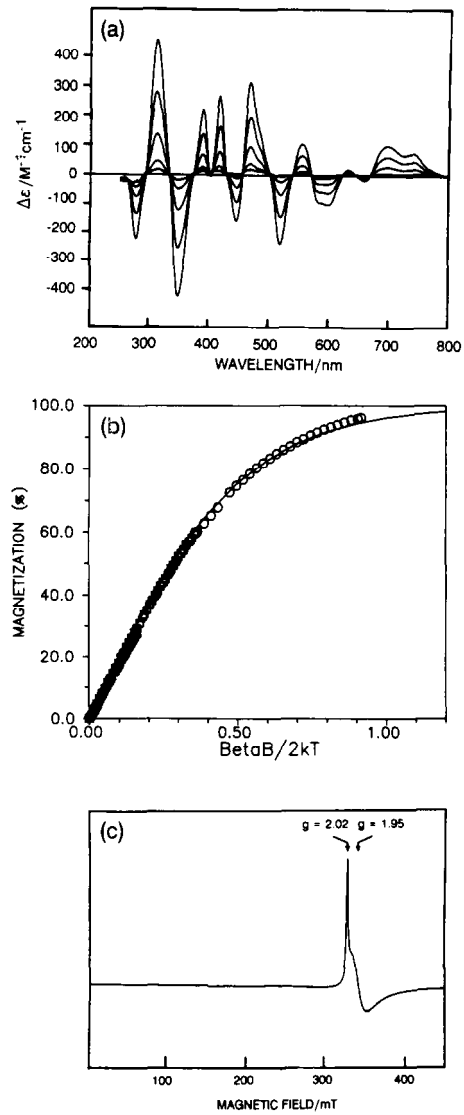

FIG. 5. **Variable temperature MCD spectra, MCD magnetization plot, and EPR spectrum of ferricyanide-oxidized *P. furiosus* ferredoxin.** Anaerobically purified *P. furiosus* ferredoxin was incubated with a 5-fold excess of potassium ferricyanide at room temperature for 15 min and repurified using a Sephadex G-25 column. Sample (0.25 mM) is in 50 mM Tris/HCl buffer (pH 7.8) with 50% (v/v) glycerol. *a*, variable temperature MCD spectra at 4.5 T and 1.59 K, 4.22 K, 9.9 K, 17.6 K, and 53 K (MCD intensity at all wavelengths increases with decreasing temperature). *b*, MCD magnetization data at 464 nm. Magnetic fields between 0 and 4.5 T; temperatures: O, 1.66 K; □, 4.22 K; △, 9.4 K. *Solid line* is theoretical magnetization data for $g_{\parallel} = 2.02$, $g_{\perp} = 1.95$, polarization ratio, $m_z/m_{x,y} = -1$, computed using Equation 1 of Ref. 22. *c*, EPR spectrum. Conditions of measurement: microwave power, 1 mW; temperature 8 K; modulation amplitude, 0.63 mT; microwave frequency, 9.42 GHz.

Fig. 6 shows variable temperature MCD spectra and magnetization data and the EPR spectrum of ferricyanide-oxidized *P. furiosus* Fd after removal of the excess oxidant by gel filtration and reduction with sodium dithionite. Based on the low temperature MCD spectra reported for ferredoxins containing reduced [3Fe-4S] centers (23–27), the form and intensity of the temperature-dependent MCD spectrum shown in Fig. 6*a* are entirely consistent with one [3Fe-4S]^{0} cluster. The MCD magnetization data collected for the band at 704 nm are well fit at the lowest temperature (1.61 K) by theoretical data constructed for a ground state doublet with $g_{\parallel} = 8.0$ and $g_{\perp} = 0.0$ (see Fig. 6*b*). This behavior is indicative of an $S = 2$ ground state with negative axial zero-field splitting

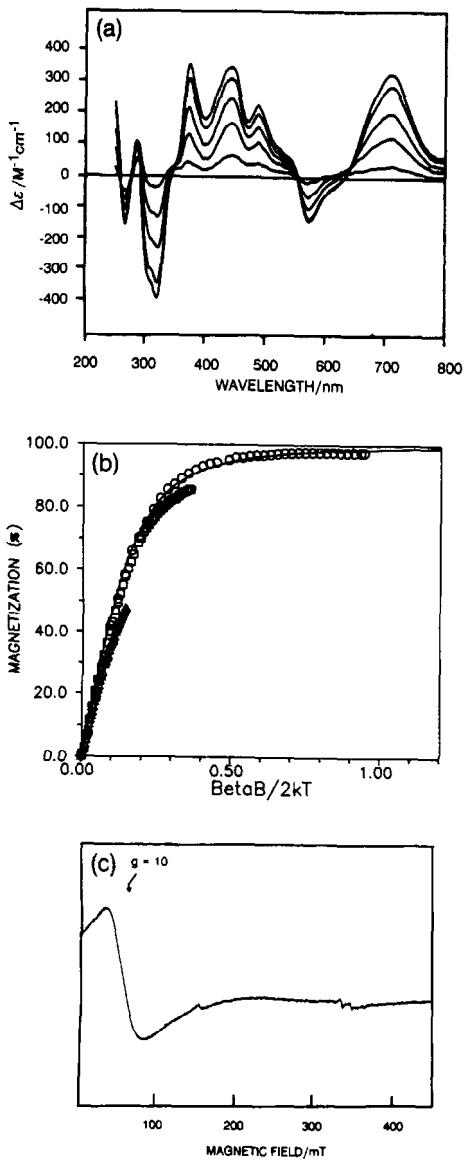

FIG. 6. **Variable temperature MCD spectra, MCD magnetization plot, and EPR spectrum of dithionite-reduced ferricyanide-oxidized *P. furiosus* ferredoxin.** Sample is the same as that described in Fig. 5, except for reduction by addition of sodium dithionite (2 mM) after anaerobic repurification. *a*, variable temperature MCD spectra at 4.5 T and 1.67 K, 4.22 K, 9.0 K, 15.8 K, and 51 K (MCD intensity at all wavelengths increases with decreasing temperature). *b*, MCD magnetization data at 704 nm. Magnetic fields between 0 and 4.5 T; temperatures: O, 1.61 K; □, 4.22 K; Δ, 10.6 K. *Solid line* is theoretical magnetization data for $g_{\parallel} = 8.0$, $g_{\perp} = 0.0$, computed using Equation 3 of Ref. 22. *c*, EPR spectrum. Conditions of measurement: microwave power, 50 mW; temperature, 8 K; modulation amplitude, 0.63 mT; microwave frequency, 9.41 GHz.

leaving an $M_S = \pm 2$ doublet lowest in energy. Such ground state magnetic properties are a common attribute of all known $[3Fe\text{-}4S]^0$ clusters (23–27). The low temperature MCD spectrum of the $[3Fe\text{-}4S]^0$ cluster in *P. furiosus* Fd was found to be invariant to pH in the range 6–9. In contrast, the $[3Fe\text{-}4S]^0$ clusters in *A. vinelandii* and *Azotobacter chroococcum* ferredoxins have been shown to undergo cluster protonation with a $pK_a \sim 7.8$ which is manifest by a dramatic change in the low temperature MCD spectrum (23, 27). However, this is not a general property of $[3Fe\text{-}4S]^0$ clusters and is not observed for *T. thermophilus* and *D. gigas* Fds in addition to *P. furiosus* Fd.

Likewise, the *X*-band EPR spectral properties of the $[3Fe\text{-}4S]^0$ cluster in *P. furiosus* Fd (see Fig. 6*c*) are analogous to those in *T. thermophilus* and *D. gigas* Fds and distinct from *A. vinelandii* Fd. The EPR spectrum consists of a broad derivative-shaped feature centered at $g = 10$ which increases in intensity with decreasing temperature over the range 30–4.2 K. Very similar resonances have been reported for reduced *T. thermophilus* and *D. gigas* Fds and assigned to transitions within the lowest $M_S = \pm 2$ doublet of the $S = 2$ ground state (28, 29). The absence of such EPR signals in reduced *A. vinelandii* Fd has been attributed to a larger rhombic zero-field splitting of the $M_S = \pm 2$ doublet such that resonance is not possible with *X*-band microwave radiation (23).

The MCD and EPR results taken together show quantitative one electron reduction of the [3Fe-4S] cluster in ferricyanide-oxidized *P. furiosus* Fd without significant reconversion to a [4Fe-4S] cluster. However, quantitative cluster conversion is readily accomplished by adding stoichiometric amounts of Fe(II) ions under reducing conditions. The resulting samples exhibited EPR spectra identical to those shown in Fig. 1 for the dithionite-reduced anaerobically prepared ferredoxin (data not shown).

Aerobically Purified Ferredoxin

As Prepared—The aerobically purified ferredoxin exhibited MCD and EPR spectra closely resembling those of the $[3Fe\text{-}4S]^+$ cluster in the ferricyanide-oxidized anaerobic sample shown in Fig. 5 (data not shown). The EPR signal accounted for 0.28 spins/molecule (see Table II), and the MCD spectrum was approximately one-third of the intensity of that shown in Fig. 5*a* under comparable conditions. The resonance Raman spectrum provides definitive evidence that the aerobic preparations are heterogeneous in terms of cluster composition (see Fig. 4*c*). Raman bands attributable to EPR- and MCD-detectable $S = 1/2$ $[3Fe\text{-}4S]^+$ clusters as well as diamagnetic ($S = 0$) $[4Fe\text{-}4S]^{2+}$ clusters are readily discernible. The spectrum of the latter appears to be identical to that of $[4Fe\text{-}4S]^{2+}$ centers in the thionine- or air-oxidized anaerobically prepared ferredoxin, and subtraction of this component affords the resonance Raman spectrum of the $[3Fe\text{-}4S]^+$ centers in the aerobically prepared sample (see Fig. 4*d*). The resulting spectrum is typical of that observed for bacterial $[3Fe\text{-}4S]^+$ centers (see above). However, it does show differences, particularly in the frequency of the two lowest energy Fe-S bridging modes and the relative intensities of the bands, compared with the $[3Fe\text{-}4S]^+$ cluster generated by ferricyanide oxidation of the $[4Fe\text{-}4S]^{2+}$ cluster in the anaerobically prepared ferredoxin (cf. Fig. 4, *b* and *d*), suggesting small but significant structural differences in the [3Fe-4S] core structures. This result is surprising in light of the identical EPR and MCD characteristics of the $[3Fe\text{-}4S]^+$ clusters in these samples. An alternative explanation of the Raman results is that an additional Fe-S cluster with dominant bands at 286 and 395 cm^{-1} (and possibly 269 cm^{-1}) is present in the aerobically prepared samples. As discussed below, there is EPR evidence for an additional minor species in reduced samples.

Dithionite-reduced—The EPR and variable temperature MCD spectra for dithionite-reduced samples of the aerobically purified ferredoxin closely resemble those shown in Figs. 1 and 3, respectively (data not shown). Spin quantitations were carried out for the MCD samples that contained 50% (v/v) glycerol. The combined quantitation of the $S = 1/2$ and $S = 3/2$ resonances corresponds to approximately 80% of that obtained for the equivalent anaerobically prepared samples, and the ratio of the $S = 1/2$ to $S = 3/2$ species is in good agreement (see Table II). No evidence for any residual $S = 2$

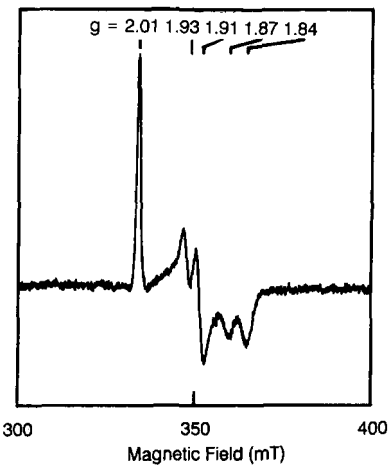

FIG. 7. **The novel $S = 1/2$ EPR signals in dithionite-reduced aerobically purified *P. furiosus* ferredoxin.** Aerobically purified ferredoxin (0.28 mM) in 50 mM Tris/HCl buffer (pH 7.8) reduced with 2 mM sodium dithionite. Conditions of measurement: microwave power, 1 mW; temperature, 30 K; modulation amplitude, 0.5 mT; microwave frequency, 9.41 GHz.

$[3Fe\text{-}4S]^0$ centers was apparent in either the MCD or EPR spectra, indicating that the samples had sufficient adventitious iron to effect complete [3Fe-4S] to [4Fe-4S] conversion. However, all samples from two independent aerobic purifications exhibited additional $S = 1/2$ EPR signals from slow relaxing species which were still apparent without sufficient broadening at 100 K. These new resonances are shown in Fig. 7 at 30 K and 1-mW microwave power. Under these conditions, the fast relaxing underlying $S = 1/2$ resonance (g = 2.10, 1.87, 1.80) is not observed due to relaxation broadening. Microwave power and temperature studies suggest that the signal results from two overlapping resonances with g = 2.01, 1.91, 1.84 and g = 2.01, 1.93, 1.87, with the former being the faster relaxing species. Together these resonances account for 0.10 spins/molecule. Although the g-values and relaxation properties of these $S = 1/2$ resonances more closely resemble those observed for $[2Fe\text{-}2S]^+$ clusters than $[4Fe\text{-}4S]^+$ clusters, analogus spectra have not been observed for any Fe-S protein.

DISCUSSION

The spectroscopic results presented above provide unambiguous evidence for a single $[4Fe\text{-}4S]^{+,2+}$ cluster in aerobically isolated *P. furiosus* Fd. Prolonged exposure to oxygen during aerobic isolation results in partial (~30%) [4Fe-4S] to [3Fe-4S] cluster degradation. However, once isolated under anaerobic conditions, the [4Fe-4S] cluster is remarkably inert to aerial degradation. Most likely the sensitivity to oxygen is a consequence of perturbations to the polypeptide structure resulting from high ionic strengths and/or binding to an anion exchange resin. Facile and quantitative [4Fe-4S] to [3Fe-4S] cluster conversion is, however, accomplished by oxidation with a small excess (5-fold) of potassium ferricyanide, and the reverse process proceeds readily upon incubation with Fe(II) under reducing conditions. This cluster interconversion occurs more readily than in *D. gigas* Fd (30), and the ease with which it occurs is comparable to that in aconitase (31). These results suggest that only the [4Fe-4S] form exists *in vivo*, and in accord with this conclusion, the [3Fe-4S] form is much less effective in transferring electrons to the hydrogenase of this organism *in vitro*.[6]

The combination of resonance Raman, MCD, and EPR spectroscopies show that the $[3Fe\text{-}4S]^{+,0}$ cluster has unremarkable properties in both the oxidized and reduced states and is quite comparable with similar clusters in ferredoxins from *D. gigas*, *T. thermophilus*, and *C. pasteurianum*. In contrast the $[4Fe\text{-}4S]^{+,2+}$ cluster has anomalous spectroscopic properties in both the oxidized and reduced states, implying non-cysteinyl coordination for the iron atom that is incorporated in [3Fe-4S] to [4Fe-4S] conversion.

The $[4Fe\text{-}4S]^+$ cluster in *P. furiosus* Fd exists with a mixture of $S = 1/2$ and $S = 3/2$ ground states, as opposed to the $S = 1/2$ $[4Fe\text{-}4S]^+$ centers that are generally found in reduced bacterial ferredoxins. Indeed the majority of the clusters (>80%) have $S = 3/2$ ground states under the conditions used in these investigations. The question that needs to be addressed is whether the novel ground state spin properties are a direct consequence of non-cysteinyl coordination of a specific iron atom. As discussed below, the currently available data suggest that non-cysteinyl ligation of one iron atom is neither necessary nor sufficient to produce $S = 3/2$ spin states for biological $[4Fe\text{-}4S]^+$ clusters.

Biological $[4Fe\text{-}4S]^+$ clusters with $S = 3/2$ ground states have been identified in a variety of different Fe-S enzymes; nitrogenase Fe-protein (32–34), amidotransferase from *Bacillus subtilis* (35), and hydrogenase I from *C. pasteurianum* (12). Although the nature of the ligands binding the $S = 3/2$ cluster is unknown in the case of hydrogenase I, there is evidence for complete cysteinyl coordination in the other two enzymes. In addition to the resonance Raman data for both enzymes (see below), the number and Fd-type arrangement of cysteine residues in *B. subtilis* amidotransferase (35, 36) and the studies of nitrogenase Fe-proteins with site-mutated or chemically modified cysteinyl residues (37, 38) argue in favor of complete cysteinyl coordination. Furthermore, studies of synthetic analog clusters of the type $[Fe_4S_4(SR)_4]^{3-}$ (R = alkyl or aryl group) show that all exist as mixtures of $S = 1/2$ or $3/2$ spin states in frozen acetonitrile or dimethylformamide solutions (39). Although a structural basis for the predominance of $S = 3/2$ or $S = 1/2$ ground states has yet to emerge (39–41), it is clear from these considerations that non-cysteinyl coordination of a specific iron atom is not a requirement for biological $[4Fe\text{-}4S]^+$ clusters to adopt $S = 3/2$ ground states.

Evidence that non-cysteinyl coordination of a specific iron atom does not always result in $S = 3/2$ $[4Fe\text{-}4S]^+$ clusters is provided by aconitase. Recent x-ray crystallographic studies have shown that the $[4Fe\text{-}4S]^{2+}$ cluster in active aconitase has water or hydroxide as the terminal ligand to the iron atom that is inserted during the activation procedure, with cysteines 359, 422, and 425 coordinating the remaining iron atoms (9, 42). Moreover the combination of EPR, electron nuclear double resonance, and Mössbauer spectroscopies has shown that substrate and inhibitors bind to the unique iron site of the $[4Fe\text{-}4S]^+$ cluster (10). However, although the EPR spectrum of the $[4Fe\text{-}4S]^+$ cluster in reduced active aconitase is extremely sensitive to the binding of citrate or inhibitors such as *trans*-aconitate, only $S = 1/2$ resonances have been observed (10, 43). This has been confirmed by recent variable temperature MCD and EPR studies of reduced active aconitase in the presence and absence of citrate and *trans*-aconitate, which specifically looked for evidence of $S = 3/2$ species.[7]

Thus far the discussion has considered $S = 3/2$ $[4Fe\text{-}4S]^+$ centers as a generic species. However, it is clear that in different proteins they differ in terms of their ground state zero-field splitting parameters and the extent to which the $S = 1/2$ and $S = 3/2$ spin mixture is perturbed by medium

[6] J.-B. Park and M. W. W. Adams, unpublished observations.

[7] M. T. Werth, A. T. Kowal, M. K. Johnson, M. C. Kennedy, and H. Beinert, unpublished results.

effects. The $S = 3/2$ clusters in nitrogenase Fe-proteins and *C. pasteurianum* hydrogenase I exhibit very similar ground state properties, $E/D = 0.22$ and $D = -2.5$ cm^{-1} (27) and $E/D = 0.15$ and $D = -2.8$ cm^{-1} (12), respectively, that are quite distinct from those of the clusters in *B. subtilis* amidotransferase, $E/D \sim 0$ and $D > 0$ (35), or *P. furiosus* Fd, $E/D = 0.22$ and $D = +3.3$ cm^{-1}. The spin mixture in nitrogenase Fe-proteins is very dependent on the nature of the medium. The addition of glassing agents such as glycerol and ethylene glycol to 50% (v/v) results in samples in which 90% of the clusters are in the $S = 1/2$ form, whereas denaturing agents such as 0.4 M urea result in 85% of the clusters being in an $S = 3/2$ form (32–34). In contrast, the spin mixture in *P. furiosus* Fd is relatively insensitive to the medium with 0.4 M urea inducing no change, and 50% (v/v) glycerol resulting in a slight shift in favor of the $S = 3/2$ form. We conclude that the properties of the $S = 3/2$ [4Fe-4S]$^+$ clusters in *P. furiosus* Fd are quite distinct from those in other proteins.

It is possible that the unique properties of the $S = 3/2$ [4Fe-4S]$^+$ center in *P. furiosus* Fd are specific to clusters in which one iron atom is coordinated by an aspartic acid residue. Although the ligation of the unique iron atom is not definitively known, several pieces of evidence argue in favor of aspartic acid coordination rather than H_2O or OH^- coordination, which are the only logical alternatives. First, in aconitase in which H_2O or OH^- coordination of one iron atom has been established by x-ray crystallographic studies (9), the reduced cluster exhibits an $S = 1/2$ ground state exclusively. Second, the invariance of the EPR and low temperature MCD spectra and the cluster midpoint potential[5] over the range pH 6.0–10.5 is inconsistent with H_2O coordination. However, it is possible that OH^- coordinates to the cluster and remains unprotonated over this entire pH range. Based on these considerations, we conclude that aspartate coordination is most likely, although we cannot rule out OH^- or aspartate and OH^- coordination for the unique iron atom.

Support for the hypothesis that the novel ground state properties are a direct consequence of having an aspartic acid residue at position 14 in place of the conventional cysteine residue comes from spectroscopic studies of the 8Fe form of *D. africanus* FdIII (44), which appeared in the literature just prior to submission of this manuscript. This ferredoxin contains only 7 cysteine residues, and the sequence has been determined (4). Four of the cysteine residues are in a typical [4Fe-4S]-Fd arrangement, and the remaining 3 are arranged in the same way as the coordinating cysteinyl residues in *P. furiosus* Fd, with an aspartic acid residue again in place of the cysteinyl residue that would customarily be involved in cluster ligation. As isolated under aerobic conditions, this ferredoxin contains both [4Fe-4S]$^{2+,+}$ and [3Fe-4S]$^{+,0}$ (45), but the latter readily takes up a Fe(II) ion under reducing conditions to give a second [4Fe-4S]$^{2+,+}$ with non-cysteinyl coordination of the incorporated iron atom. The authors present arguments in favor of aspartic acid coordination of this iron atom. However, as discussed above for *P. furiosus* Fd, OH^- coordination cannot be ruled out by the data presented. Based on a comparison of their EPR and variable temperature MCD characteristics, the electronic and magnetic properties of the novel [4Fe-4S]$^+$ clusters in these two ferredoxins are strikingly similar. Both have predominantly $S = 3/2$ ground states, with comparable EPR spectra. The cluster in *D. africanus* FdIII has slightly greater rhombicity ($E/D \sim 0.27$) that precludes detection of distinct EPR resonances from both doublets and hence estimation of the zero-field splitting.

In common with all known [4Fe-4S]$^{2+}$ clusters, the [4Fe-4S]$^{2+}$ in oxidized *P. furiosus* Fd is diamagnetic at liquid helium temperatures, indicating an $S = 0$ ground state. However, the resonance Raman spectra reported above reveal anomalous structural properties for the [4Fe-4S]$^{2+}$ cluster in *P. furiosus* Fd. The most significant difference lies in the frequency of the totally symmetric bridging vibration, which is the dominant feature in the Raman spectrum. Table III compares this frequency for a wide range of biological [4Fe-4S]$^{2+}$ clusters and an appropriate synthetic analog. (Some of the proteins listed contain [4Fe-4S]$^{2+}$ and [3Fe-4S]$^+$ clusters. However, the frequencies given are specific to the [4Fe-4S]$^{2+}$ centers.) The data are organized in two groups. The first group contains clusters for which there is evidence for complete cysteinyl (or thiolate) coordination from x-ray crystallographic studies, sequence comparison with simple structurally characterized ferredoxins, or chemical modification and site-specific mutation of specific cysteine residues. The totally symmetric bridging frequencies span 333–338 cm^{-1} for this group. The second group consists of the three well authenticated examples of biological [4Fe-4S]$^{2+}$ clusters that are site differentiated via anomalous coordination of a specific iron atom, *i.e.* aconitase, *Escherichia coli* sulfite reductase hemoprotein, and *P. furiosus* Fd. The nature of the ligand that bridges between the siroheme iron and one of the iron atoms of the [4Fe-4S] cluster in the sulfite reductase hemoprotein is not known definitively, although recent resonance Raman results argue in favor of a bridging thiolate (46). The totally symmetric bridging frequencies for this group are quite distinct from the first group and span 340–342 cm^{-1}. Although a detailed rationalization of this phenomenon has yet to emerge, it most likely reflects the lowering of the effective cluster symmetry to C_{3v} via the unique coordination of a specific iron, and hence a shift in frequencies toward those of the [3Fe-4S]$^+$ cluster (46). The comparable band for [3Fe-4S]$^+$ clusters in bacterial ferredoxins is at 347–348 cm^{-1} (21). These results suggest that the frequency of the totally symmetric bridging vibration is a useful indicator of site differentiation in [4Fe-4S]$^{2+}$ clusters arising from differences in iron ligation.

Finally, we turn our attention to the origin of the novel $S = 1/2$ EPR signals that are observed as minor species only in

TABLE III

Comparison of the totally symmetric Fe-S bridging stretching frequencies (ν(Fe-S$_b$)) for biological and synthetic [4Fe-4S]$^{2+}$ clusters

See Footnote 3.

	ν(Fe-S$_b$)	Ref.
Clusters with complete cysteinyl (or thiolate) coordination	cm^{-1}	
B. subtilis amidotransferase	333	35
A. vinelandii FdI	334	21
T. thermophilus Fd	334	21
C. pasteurianum nitrogenase Fe-protein	334	[a]
A. vinelandii nitrogenase Fe-protein	335	47
[Fe$_4$S$_4$(SCH$_2$Ph)$_4$]$^{3-}$ (dimethylacetamide solution)	336	20
D. gigas hydrogenase	337	[b]
C. vinosum HiPIP[c]	337	20
C. pasteurianum Fd	338	20
Clusters with anomalous coordination of a specific iron atom		
Active beef heart aconitase	340	[d]
E. coli sulfite reductase hemoprotein	342	46
P. furiosus Fd	342	This work

[a] W. Fu, T. V. Morgan, and M. K. Johnson, unpublished results.
[b] P. M. Drozdzewski, J. LeGall, and M. K. Johnson, unpublished results.
[c] HiPIP, high potential iron-sulfur protein.
[d] T. G. Spiro, personal communication. This frequency is invariant to the binding of citrate, nitroisocitrate, or *trans*-aconitate to the cluster.

dithionite-reduced aerobic preparations. These resonances could conceivably arise from O_2 binding to the unique iron site of the cluster. Precedent for O_2 binding to an Fe-S cluster is provided by the novel H_2-activating cluster in *C. pasteurianum* hydrogenase I (48). However, we have not observed similar EPR signals in dithionite-reduced anaerobically prepared samples that were oxidized with air and saturated with O_2 prior to re-reduction. A more likely explanation, in view of the relatively slow relaxation properties of these resonances, is that they arise from $[2Fe\text{-}2S]^+$ clusters. Precedent for oxidative degradation of $[4Fe\text{-}4S]^{2+}$ clusters to yield $[2Fe\text{-}2S]^{2+}$ clusters is provided by nitrogenase iron protein (49). Tentative support for this interpretation is provided by the resonance Raman spectrum of the aerobically prepared ferredoxin. Biological $[2Fe\text{-}2S]^{2+}$ clusters have a prominent Raman band between 282 and 291 cm^{-1}, 329 and 349 cm^{-1}, and 387 and 395 cm^{-1} with 457.9 nm excitation (50). With this in mind, comparison of the Raman spectra attributed to the $[3Fe\text{-}4S]^+$ clusters in ferricyanide-treated anaerobic preparations and in aerobic preparations (Fig. 4, *b* and *d*), respectively, suggests that the latter may also contain contributions from a $[2Fe\text{-}2S]^{2+}$ center.

REFERENCES

1. Aono, S., Bryant, F. O., and Adams, M. W. W. (1989) *J. Bacteriol.* **171,** 3433–3439
2. Bruschi, M., and Guerlesquin, F. (1988) *FEMS Microbiol. Rev.* **54,** 155–176
3. Okawara, N., Ogata, M., Yagi, T., Wakabayashi, S., and Matsubara, H. (1988) *J. Biochem.* **104,** 196–199
4. Bovier-Lapierre, G., Bruschi, M., Bonicel, J., and Hatchikian, E. C. (1987) *Biochim. Biophys. Acta* **913,** 20–26
5. Wakabayashi, S., Fujimoto, N., Wada, K., Matsubara, H., Kerscher, L., and Oesterhelt, D. (1983) *FEBS Lett.* **162,** 21–24
6. Minami, Y., Wakabayashi, S., Wada, K., Matsubara, H., Kersher, L., and Oesterhelt, D. (1983) *J. Biochem.* **97,** 745–753
7. Stack, T. D. P., and Holm, R. H. (1987) *J. Am. Chem. Soc.* **109,** 2546–2547
8. Stack, T. D. P., and Holm, R. H. (1988) *J. Am. Chem. Soc.* **110,** 2484–2494
9. Robbins, A. H., and Stout, C. D. (1989) *Proc. Natl. Acad. Sci. U. S. A.* **86,** 3639–3643
10. Emptage, M. H. (1988) in *Metal Clusters in Proteins* (Que, J., Jr., ed) ACS Symposium Series Vol. 372, pp. 343–371, American Chemical Society, Wash., D. C.
11. Zimmermann, R., Münck, E., Brill, W. J., Shah, V. K., Henzl, M. T., Rawlings, J., and Orme-Johnson, W. H. (1978) *Biochim. Biophys. Acta* **537,** 185–207
12. Zambrano, I. C., Kowal, A. T., Mortenson, L. E., Adams, M. W. W., and Johnson, M. K. (1989) *J. Biol. Chem.* **264,** 20974–20983
13. Lowry, O. H., Rosebrough, N. J., Farr, A. L., and Randall, R. J. (1951) *J. Biol. Chem.* **193,** 265–275
14. Johnson, M. K. (1988) in *Metal Clusters in Proteins* (Que, J., Jr., ed) ACS Symposium Series Vol. 372, pp. 326–342, American Chemical Society, Wash., D. C.
15. Aasa, R., and Vänngård, T. (1975) *J. Magn. Res.* **19,** 308–315
16. Hamilton, C. L., Scott, R. A., and Johnson, M. K. (1989) *J. Biol. Chem.* **264,** 11650–11613
17. Hoffman, B. M., Weschler, C. J., and Basolo, F. (1976) *J. Am. Chem. Soc.* **98,** 5473–5482
18. Finnegan, M. G., Onate, Y. A., Hales, B. J., Switzer, R. L., and Johnson, M. K. (1989) *J. Inorg. Biochem.* **36,** 251
19. Spiro, T. G., Czeruszewicz, R. S., and Han, S. (1988) in *Biological Applications of Raman Spectroscopy* (Spiro, T. G., ed) Vol. 3, pp. 523–553, Wiley-Interscience, New York
20. Czernuszewicz, R. S., Macor, K. A., Johnson, M. K., Gewirth, A., and Spiro, T. G. (1987) *J. Am. Chem. Soc.* **109,** 7178–7187
21. Johnson, M. K., Czernuszewicz, R. S., Spiro, T. G., Fee, J. A., and Sweeney, W. V. (1983) *J. Am. Chem. Soc.* **105,** 6671–6678
22. Bennett, D. E., and Johnson, M. K. (1987) *Biochim. Biophys. Acta* **911,** 71–80
23. Johnson, M. K., Bennett, D. E., Fee, J. A., and Sweeney, W. V. (1987) *Biochim. Biophys. Acta* **911,** 81–94
24. Beinert, H., and Thomson, A. J. (1983) *Arch. Biochem. Biophys.* **222,** 333–361
25. Thomson, A. J., Robinson, A. E., Johnson, M. K., Moura, J. J. G., Moura, I., Xavier, A. V., and LeGall, J. (1981) *Biochim. Biophys. Acta* **670,** 93–100
26. Thomson, A. J., Robinson, A. E., Johnson, M. K., Cammack, R., Rao, K. K., and Hall, D. O. (1981) *Biochim. Biophys. Acta* **637,** 423–432
27. George, S. J., Richards, A. J. M., Thomson, A. J., and Yates, M. G. (1984) *Biochem. J.* **224,** 247–251
28. Hagen, W. R., Dunham, W. R., Johnson, M. K., and Fee, J. A. (1985) *Biochim. Biophys. Acta* **828,** 369–374
29. Papaefthymiou, V., Girerd, J.-J., Moura, I., Moura, J. J. G., and Münck, E. (1987) *J. Am. Chem. Soc.* **109,** 4703–4710
30. Moura, J. J. G., Moura, I., Kent, T. A., Lipscomb, J. D., Huynh, B. H., LeGall, J., Xavier, A. V., and Münck, E. (1982) *J. Biol. Chem.* **257,** 6259–6267
31. Kent, T. A., Dreyer, J.-L., Kennedy, M. C., Huynh, B. H., Emptage, M. H., Beinert, H., and Münck, E. (1982) *Proc. Natl. Acad. Sci. U. S. A.* **79,** 1096–1100
32. Lindahl, P. A., Day, E. P., Kent, T. A., Orme-Johnson, W. H., and Münck, E. (1985) *J. Biol. Chem.* **260,** 11160–11173
33. Hagen, W. R., Eady, R. R., Dunham, W. R., and Haaker, H. (1985) *FEBS Lett.* **189,** 250–254
34. Watt, G. D., and McDonald, J. W. (1985) *Biochemistry* **24,** 7226–7231
35. Onate, Y. A., Vollmer, S. J., Switzer, R. L., and Johnson, M. K. (1989) *J. Biol. Chem.* **264,** 18386–18391
36. Makaroff, C. A., Zalkin, H., Switzer, R. L., and Vollmer, S. J. (1983) *J. Biol. Chem.* **258,** 10586–10593
37. Hausinger, R. P., and Howard, J. B. (1983) *J. Biol. Chem.* **258,** 13486–13492
38. Howard, J. B., Davis, R., Moldenhauer, B., Cash, V. L., and Dean, D. (1989) *J. Biol. Chem.* **264,** 11270–11274
39. Carney, M. J., Papaefthymiou, G. C., Spartalian, K., Frankel, R. B., and Holm, R. H. (1988) *J. Am. Chem. Soc.* **110,** 6084–6095
40. Carney, M. J., Papaefthymiou, G. C., Frankel, R. B., and Holm, R. H. (1989) *Inorg. Chem.* **28,** 1497–1503
41. Lindahl, P. A., Teo, B-K., and Orme-Johnson, W. H. (1987) *Inorg. Chem.* **26,** 3912–3916
42. Robbins, A. H., and Stout, C. D. (1989) *Proteins Struct. Funct. Genet.* **5,** 289–312
43. Emptage, M. H., Dreyer, J.-L., Kennedy, M. C., and Beinert, H. (1983) *J. Biol. Chem.* **258,** 11106–11111
44. George, S. J., Armstrong, F. A., Hatchikian, E. C., and Thomson, A. J. (1989) *Biochem. J.* **264,** 275–284
45. Armstrong, F. A., George, S. J., Cammack, R., Hatchikian, E. C., and Thomson, A. J. (1989) *Biochem. J.* **264,** 265–273
46. Madden, J. F., Han, S., Siegel, L. M., and Spiro, T. G. (1989) *Biochemistry* **28,** 5471–5477
47. Onate, Y. A. (1989) *Spectroscopic Studies of Biological and Synthetic [4Fe-4S] Clusters.* Ph.D. thesis, Louisiana State University, Baton Rouge
48. Kowal, A. T., Adams, M. W. W., and Johnson, M. K. (1989) *J. Biol. Chem.* **264,** 4342–4348
49. Anderson, G. L., and Howard, J. B. (1984) *Biochemistry* **23,** 2118–2122
50. Han, S., Czernuszewicz, R. S., Kimura, T., Adams, M. W. W., and Spiro, T. G. (1989) *J. Am. Chem. Soc.* **111,** 3505–3511